

## NRC Publications Archive Archives des publications du CNRC

### Non-grey gas radiative transfer analyses using the statistical narrow-band model

Liu, Fengshan; Gulder, O. L.; Smallwood, Gregory; Ju, Y.

This publication could be one of several versions: author's original, accepted manuscript or the publisher's version. / La version de cette publication peut être l'une des suivantes : la version prépublication de l'auteur, la version acceptée du manuscrit ou la version de l'éditeur.

For the publisher's version, please access the DOI link below. / Pour consulter la version de l'éditeur, utilisez le lien DOI ci-dessous.

#### **Publisher's version / Version de l'éditeur:**

[https://doi.org/10.1016/S0017-9310\(97\)00267-6](https://doi.org/10.1016/S0017-9310(97)00267-6)

*International Journal of Heat & Mass Transfer*, 41, July 14, pp. 2227-2236, 1998-08-05

#### **NRC Publications Archive Record / Notice des Archives des publications du CNRC :**

<https://nrc-publications.canada.ca/eng/view/object/?id=6fe6a7cd-610f-4b04-a0a7-6e5b4d8e2eda>

<https://publications-cnrc.canada.ca/fra/voir/objet/?id=6fe6a7cd-610f-4b04-a0a7-6e5b4d8e2eda>

Access and use of this website and the material on it are subject to the Terms and Conditions set forth at

<https://nrc-publications.canada.ca/eng/copyright>

READ THESE TERMS AND CONDITIONS CAREFULLY BEFORE USING THIS WEBSITE.

L'accès à ce site Web et l'utilisation de son contenu sont assujettis aux conditions présentées dans le site

<https://publications-cnrc.canada.ca/fra/droits>

LISEZ CES CONDITIONS ATTENTIVEMENT AVANT D'UTILISER CE SITE WEB.

**Questions?** Contact the NRC Publications Archive team at

PublicationsArchive-ArchivesPublications@nrc-cnrc.gc.ca. If you wish to email the authors directly, please see the first page of the publication for their contact information.

**Vous avez des questions?** Nous pouvons vous aider. Pour communiquer directement avec un auteur, consultez la première page de la revue dans laquelle son article a été publié afin de trouver ses coordonnées. Si vous n'arrivez pas à les repérer, communiquez avec nous à PublicationsArchive-ArchivesPublications@nrc-cnrc.gc.ca.



PII: S0017-9310(97)00267-6

# Non-grey gas radiative transfer analyses using the statistical narrow-band model†

F. LIU,‡ Ö. L. GÜLDER and G. J. SMALLWOOD

Combustion Research, Institute for Chemical Process and Environmental Technology, National Research Council, Montreal Road, Ottawa, Ontario, Canada K1A 0R6

and

Y. JU

Department of Aeronautics and Space Engineering, Tohoku University, Aoba-ku, Sendai 980, Japan

(Received 10 April 1997 and in final form 29 August 1997)

**Abstract**—Nongrey gas radiation analyses were conducted using the statistical narrow-band model and four implementation methods: the exact or the correlated formulation, the noncorrelated expression, grey-band approximation based on global absorption coefficient, and a new approximate method. The new method is also a grey-band approximation but utilizes the local absorption coefficient. Using results of the correlated formulation as benchmark solution, accuracy of the three approximate narrow-band implementation methods was investigated for several one-dimensional non-grey gas radiation problems in parallel plate enclosure containing radiating gases of both uniform and non-uniform temperatures and/or concentrations. Radiative source term and wall heat flux predicted by the noncorrelated expression and the new method are in very close agreement with each other and in fair to good agreement to benchmark solutions. Radiative source term calculated from the grey-band approximation based on global absorption coefficient is in serious error. CPU time saving of two orders of magnitude can be achieved by using the three approximate implementation methods, relative to the correlated formulation. The new method provides slightly better accuracy than the noncorrelated approach with additional advantages that an arbitrary solution method can be employed and less CPU time is required. © 1998 National Research Council of Canada. Published by Elsevier Science Ltd. All rights reserved.

## 1. INTRODUCTION

Radiative heat transfer is an important, often dominant, heat transfer mechanism in combustion systems such as furnaces, combustors, and large-scale jet flames. It has significant effects on chemical kinetics and flame structure through its direct impact on temperature and can cause flame extinction under certain conditions. It has been made clear that the flammability limit of a combustible mixture is fundamentally determined by radiative heat loss [1–4]. Moreover, recent studies on stretched flames found that multiple flame regimes [5] and flame bifurcations [6] can be induced through the effects of radiation and stretch. Therefore, there is a crucial need to ascertain how radiation reabsorption and non-grey radiation properties affect these phenomena [7].

The strong spectral dependency of radiative properties of radiating gases render the simple grey gas approximation or the optically thin assumption unacceptable if the quantitative effects of thermal radiation are to be evaluated. On the other hand, the line-

by-line calculation, which is the exact treatment of spectral gas radiation, requires enormous computing time and is therefore impractical for routine gas radiation analyses, even for one dimensional problems. As a consequence, narrow-band models are favoured as the standard for evaluation of other approximate radiative property models when line-by-line (LBL) calculations are infeasible [8]. The correlated- $k$  method [9, 10] provides an intermediate alternative between LBL and narrow-band models [11]. Direct application of the correlated- $k$  method to obtain total radiative quantities requires a quadrature over the absorption cross-section for each narrow-band, followed by a quadrature over all the bands. Therefore, the correlated- $k$  method is more computationally demanding than a narrow-band model. More recently, Denison and Webb [12–15] developed a spectral line based weighted-sum-of-grey-gases (SLWSSG) model applicable to non-isothermal and inhomogeneous gas mixtures. This model offers the advantages of accuracy and computational efficiency as far as the calculation of total radiative quantities is concerned. The SLWSSG model has been implemented into a general radiation simulation program [16]. It is worth noting that both the correlated- $k$  and the SLWSSG models

† NRC No. 37629.

‡ Author to whom correspondence should be addressed.



equation. De Miranda and Sacadura [23] proposed a noncorrelated expression for radiation intensity variation along a line of sight. This expression is the same as that for spectral or grey radiation intensity, since the derivation is essentially based on Beer’s law [24] which is valid for spectral or grey transmittance but not for the narrow-band averaged one. This is the origin of error when using this noncorrelated expression in non-grey radiation analyses. Although De Miranda and Sacadura [23] showed that this expression is an acceptable compromise between accuracy and computational efficiency based on their initial evaluation study, it requires further assessment, especially in multidimensions. In addition, it suffers the first difficulty of the exact implementation method mentioned earlier as the expression still utilizes transmittance and this restricts the choice of solution method. From a solution point of view, the grey-band approximation is preferred compared to the non-correlated expression since an arbitrary solution technique, such as DOM, can be readily used in multidimensions.

A new grey-band approximation method for implementing the SNB model is proposed in this work. The proposed grey-band approximation is novel in that the narrow-band averaged absorption coefficient is estimated using the local properties, rather than global ones as used by Kim *et al.* [22]. It was derived from the noncorrelated expression proposed by De Miranda and Sacadura [23] and Beer’s law. The purpose of developing this grey-band approximation is to maintain the advantage of grey-band approximation used by Kim *et al.* [22] and improve its accuracy.

The accuracy of the three approximate implementation methods of the SNB model outlined above was evaluated for four one-dimensional problems having different distributions of gas temperature and/or concentrations of radiating gases. Evaluation of these approximate implementation methods in multidimensions will be the objective of a future study. The correlated and noncorrelated narrow-band averaged RTEs were solved using a ray-tracing method described by Liu [21]. RTEs associated with the two grey-band approximations were solved using DOM [25]. Results obtained from the correlated formulation serve as the benchmark solution in the evaluation of the three approximate implementation methods of the SNB model. A quantitative comparison of CPU time required by the four implementation methods was made for different grid numbers to investigate their computational efficiency and the growth rate of CPU time with grid number.

**2. FORMULATION**

**2.1. Correlated narrow-band formulation**

The spectral RTE in absorbing and emitting media is written as [26]

$$\frac{\partial I_v}{\partial s} = -\kappa_{av}I_v + \kappa_{av}I_{bv} \tag{1}$$

The boundary spectral radiation intensity  $I_v(s_w, \Omega)$  at a diffuse wall is

$$I_v(s_w, \Omega) = \epsilon_{wv}I_{bwv} + \frac{(1-\epsilon_{wv})}{\pi} \int_{\hat{n}\cdot\Omega} \times |\hat{n}\cdot\Omega'| I_v(s_w, \Omega') d\Omega', \text{ for } \hat{n}\cdot\Omega' > 0. \tag{2}$$

When a narrow-band model (the SNB model in the present study) is used to provide the gas radiative properties, equation (1) must be averaged over a narrow-band to yield band averaged radiation intensity. The narrow-band averaged RTE has been presented by Kim *et al.* [22] for high-emissivity walls and by Menart *et al.* [27] for reflective walls. The present study focuses on problems having high-emissivity walls. Following Kim *et al.* [22], the narrow-band averaged RTE is written as

$$\begin{aligned} \frac{\partial \bar{I}_v(s, \Omega)}{\partial s} &= \left( \frac{\partial \tau_v(s' \rightarrow s)}{\partial s'} \right)_{s'=s} I_{bv}(s) \\ &+ \bar{I}_{wv}(s_w, \Omega) \frac{\partial}{\partial s} [\bar{\tau}_v(s_w \rightarrow s)] \\ &+ \int_{s_w}^{s_2} \frac{\partial}{\partial s} \left( \frac{\partial \tau_v(s' \rightarrow s)}{\partial s'} \right) \bar{I}_{bv}(s') ds'. \end{aligned} \tag{3}$$

The discretized form of equation (3) along a line of sight is given as [22]

$$\bar{I}_{v,n,i+1} = \bar{I}_{v,n,i} + (1 - \bar{\tau}_{v,n,i \rightarrow i+1}) \bar{I}_{bv,i+1/2} + \bar{C}_{v,n,i+1/2} \tag{4}$$

where

$$\begin{aligned} \bar{C}_{v,n,i+1/2} &= \bar{I}_{wv,n,1} (\bar{\tau}_{v,n,1 \rightarrow i+1} - \bar{\tau}_{v,n,1 \rightarrow i}) \\ &+ \sum_{k=1}^{i-1} [(\bar{\tau}_{v,n,k+1 \rightarrow i+1} - \bar{\tau}_{v,n,k+1 \rightarrow i}) \\ &- (\bar{\tau}_{v,n,k \rightarrow i+1} - \bar{\tau}_{v,n,k \rightarrow i})] \bar{I}_{bv,k+1/2} \end{aligned} \tag{5}$$

and the spatial discretisation index  $i = 1$  corresponds to the wall. In this correlated formulation, the narrow-band averaged radiation intensity at  $s_{i+1}$  depends not only on the local properties ( $\bar{I}_{v,n,i}$ ,  $\bar{\tau}_{v,n,i \rightarrow i+1}$ , and  $\bar{I}_{bv,i+1/2}$ ), but also on properties between  $s_1$  and  $s_i$ . This may be referred to as ‘history’ effects and it greatly increases the computing effort. The Curtis–Godson approximation is commonly used to obtain equivalent band parameters in nonisothermal and/or inhomogeneous media [20, 22].

The boundary condition for narrow-band averaged non-grey radiation intensity takes a similar form as equation (2).

Once the non-grey radiation intensity field is obtained, the total net radiative flux is calculated as

$$q(x_i) = \sum_{\text{all } \Delta v} \left( \sum_{n=1}^N \mu \bar{I}_{v,n,i} w_n \right) \Delta v \tag{6}$$

The radiative source term  $S$ , is then obtained from

$$S_r(x_{i+1/2}) = -\frac{dq}{dx} = -\frac{q_{i+1} - q_i}{x_{i+1} - x_i}. \quad (7)$$

### 2.2. Noncorrelated narrow-band formulation

Starting from equation (4) and using the following noncorrelated relationship

$$\bar{\tau}_{v,n,i \rightarrow i} = \prod_{k=1}^{i-1} \bar{\tau}_{v,n,k \rightarrow k+1}, \quad (8)$$

De Miranda and Sacadura [23] obtained the recursive form of the narrow-band averaged RTE

$$\bar{I}_{v,n,i+1} = \bar{I}_{v,n,i} \bar{\tau}_{v,n,i \rightarrow i+1} + \bar{I}_{b,v,i+1/2} (1 - \bar{\tau}_{v,n,i \rightarrow i+1}). \quad (9)$$

It is worth noting that this noncorrelated formulation is the same as the discretized RTE in integral form for spectral or grey radiation intensity as a direct consequence of using equation (8). In essence, equation (8) is based on Beer's law [24] which is valid for spectral or grey quantities. Unfortunately, the band averaged transmittance provided by the SNB model does not obey this law (see equation (16) below). Therefore, application of equation (9) to non-grey gas radiation analyses using the SNB model inevitably causes errors. On the other hand, the computing cost is significantly reduced using this noncorrelated formulation since radiation intensity at  $s_{i+1}$  is only dependent on local properties and the Curtis–Godson approximation is no longer needed [23].

### 2.3. Grey-band formulation

For grey-band calculations, the following form of equation (1) is solved [22, 28]

$$\frac{\partial \bar{I}_v(s, \Omega)}{\partial s} = -\bar{\kappa}_v(s) \bar{I}_v(s, \Omega) + \bar{\kappa}_v(s) \bar{I}_{b,v}(s). \quad (10)$$

Kim *et al.* [22] and Fiveland and Jamaluddin [28] obtained the equivalent narrow-band averaged absorption coefficient based on global properties,

$$\bar{\kappa}_v(s) = \frac{1}{\Delta v} \int_{\Delta v} \kappa_v dv \approx -\frac{\ln \bar{\tau}_v(L_m)}{L_m} \quad (11)$$

where the mean beam-length of the parallel plate enclosure is calculated as  $L_m = 1.8L$  [29]. This formulation results in an equivalent global narrow-band averaged absorption coefficient, i.e. it is a function of wavenumber but not spatial position. For non-isothermal and/or inhomogeneous systems, the Curtis–Godson approximation is used in the calculation of  $\bar{\tau}_v(L_m)$  [22]. It can be easily anticipated that extension of this formulation to multidimensions requires further *ad hoc* assumptions since the definition of an equivalent  $\bar{\tau}_v(L_m)$  in multidimensions is not straightforward.

An alternative and more sound method for estimating the narrow-band averaged absorption coefficient is proposed here. This alternative grey-band method again makes use of Beers' law. Starting

from the noncorrelated narrow-band expression, equation (9), and Beer's law

$$\bar{\tau}_{v,n,i \rightarrow i+1} = \exp(-\bar{\kappa}_v \delta s) \quad (12)$$

one obtains

$$\begin{aligned} \bar{I}_{v,n,i+1} &= \bar{I}_{v,n,i} \exp(-\bar{\kappa}_v \delta s) + \bar{I}_{b,v,i+1/2} (1 - \exp(-\bar{\kappa}_v \delta s)) \\ &\approx \bar{I}_{v,n,i} (1 - \bar{\kappa}_v \delta s) + \bar{I}_{b,v,i+1/2} \bar{\kappa}_v \delta s \end{aligned} \quad (13)$$

where  $\delta s$  is the pathlength between  $s_i$  and  $s_{i+1}$ . Rearranging equation (13) leads to equation (10). This analysis indicates that the equivalent narrow-band averaged absorption coefficient should be calculated as

$$\bar{\kappa}_v = -\frac{\ln \bar{\tau}_{v,n,i \rightarrow i+1}}{\delta s}. \quad (14)$$

However, this formulation yields a path dependent narrow-band averaged absorption coefficient which is of little use in view of the purpose of formulating a path independent absorption coefficient. An equivalent path independent narrow-band averaged local absorption coefficient can be obtained using the mean pathlength of the gas layer under consideration (between  $x_i$  and  $x_{i+1}$ )

$$\bar{\kappa}_v(x_{i+1/2}) = -\frac{\ln \bar{\tau}_v(l_m)}{l_m} \quad (15)$$

where  $l_m = 1.8(x_{i+1} - x_i)$  is the local mean pathlength. Since  $\bar{\tau}_v(l_m)$  and  $l_m$  are local properties of a gas layer (or a control volume in multi-dimensions), this formulation in general yields spatially varying narrow-band average absorption coefficient. It is expected that the grey-band approximation along with this local absorption coefficient is able to capture characteristics of non-grey radiation encountered in nonisothermal and inhomogeneous media since the local conditions are incorporated into the model. In addition, extension of equation (15) to multidimensions is straightforward since the local properties are well defined.

### 2.4. The statistical narrow-band model

In the SNB model, the narrow-band averaged transmittance for an isothermal and homogeneous path  $|s' \rightarrow s|$  is given as [30]

$$\bar{\tau}_v(s' \rightarrow s) = \exp \left[ -\frac{\bar{\beta}_v}{\pi} \left( \sqrt{1 + \frac{2\pi f p |s' \rightarrow s| \bar{\kappa}_v}{\bar{\beta}_v}} - 1 \right) \right] \quad (16)$$

where the average line-width to spacing ratio is given as  $\bar{\beta}_v = 2\pi \bar{\gamma}_v / \delta v$ . The SNB model has been extensively validated and used in non-grey gas radiation calculations [17–20, 22]. The mean narrow-band parameters  $\bar{\kappa}_v$ ,  $\bar{\gamma}_v$ , and  $1/\delta v$  for H<sub>2</sub>O and CO<sub>2</sub> in the temperature range of 300–1500 K have been reported by Hartmann *et al.* [17], Soufiani *et al.* [18], and Zhang *et al.* [19] based on line-by-line calculations. An updated data set of the SNB model parameters has been

recently made available by Soufiani and Taine [20] for  $\text{CO}_2$ ,  $\text{H}_2\text{O}$  and  $\text{CO}$  and for a much wider temperature range of 300–2900 K. This new data set is for a  $25 \text{ cm}^{-1}$  wavenumber resolution in the entire wavenumber range. Further details of this data set can be found in ref. [20]. This new data set was provided by Soufiani [31] and used in the present non-grey gas radiation analyses.

### 3. RESULTS AND DISCUSSION

The correlated and noncorrelated narrow-band averaged RTEs, equations (4) and (9), were solved using a ray-tracing method described in ref. [21]. The grey-band RTE, equation (10), was solved using DOM along with the diamond (central) spatial differencing scheme [25]. The SNB model with the updated data set was used in all the calculations for obtaining the narrow-band averaged transmittance and global and local grey-band absorption coefficients.

Numerical calculations were performed for four test cases. In all four cases, the wall surfaces were assumed to be black and the medium was at a uniform pressure of 1 atm. In the first case, the medium bounded by the two parallel plates is pure water vapour at a uniform temperature of 1000 K. The two bounding walls are cold (at 0 K). Two separation distances,  $L = 0.1 \text{ m}$  and  $1 \text{ m}$ , were considered in this case. The input parameters of the second case are the same as the first one except that the medium now is a mixture of  $\text{N}_2$  and  $\text{H}_2\text{O}$  with a parabolic  $\text{H}_2\text{O}$  concentration profile given by  $f_{\text{H}_2\text{O}} = 4(1 - x/L)x/L$  and the separation distances is  $L = 1 \text{ m}$ . In the third case, the medium is again pure  $\text{H}_2\text{O}$  with a boundary layer type temperature distribution [22]. The left wall is hot at 1500 K and the right wall is cold at 300 K. The separation distance is  $L = 0.2 \text{ m}$ . These three test cases provide good testbeds to evaluate separately the effects of pathlength and gas temperature and concentration distributions on the results and have been previously chosen as test cases by Kim *et al.* [22], Liu and Tiwari [32], De Miranda and Sacadura [23], and Denison and Webb [12] using different solution methods and/or radiative property models. The fourth case considered is a typical configuration of temperature and  $\text{CO}_2$  and  $\text{H}_2\text{O}$  concentration distributions encountered in a counterflow methane–air diffusion flame. The separation distance is  $0.5 \text{ m}$  and two bounding walls are

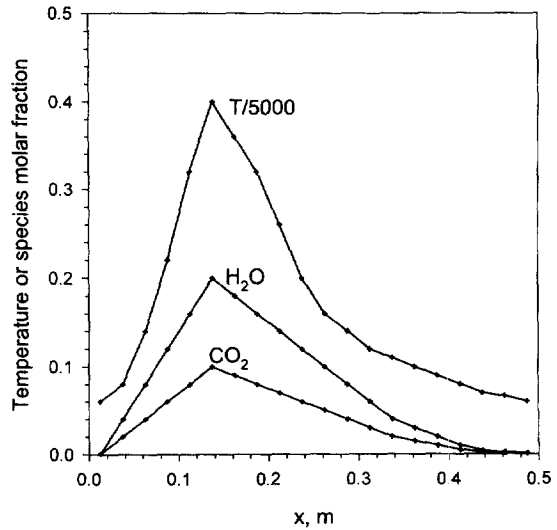


Fig. 1. Temperature and species concentration distributions of a simulated counterflow methane/air diffusion flame.

at 300 K. The medium is assumed to contain a mixture of  $\text{N}_2$ ,  $\text{CO}_2$ , and  $\text{H}_2\text{O}$ . The distribution of temperature and radiating gas concentrations is shown in Fig. 1. These conditions correspond to a thick flame which is of primary interest since for a thin flame the optically thin limit is approached. Characteristics of the four test cases are summarised in Table 1.

For all the four test cases, the one-dimensional parallel plate enclosure was divided into 20 uniform gas layers. Angular discretisation in all the four test cases was achieved using the  $T_3$  quadrature set [33]. This angular discretisation was validated as adequate, i.e. further refinement does not significantly alter the numerical results.

For convenience of discussion, the correlated formulation, the noncorrelated formulation, grey-band approximations using the global and local absorption coefficients will be named Methods I, II, III, and IV, respectively, as summarised in Table 2. Results of Method I are used as the benchmark solution to check the accuracy of the three approximate methods.

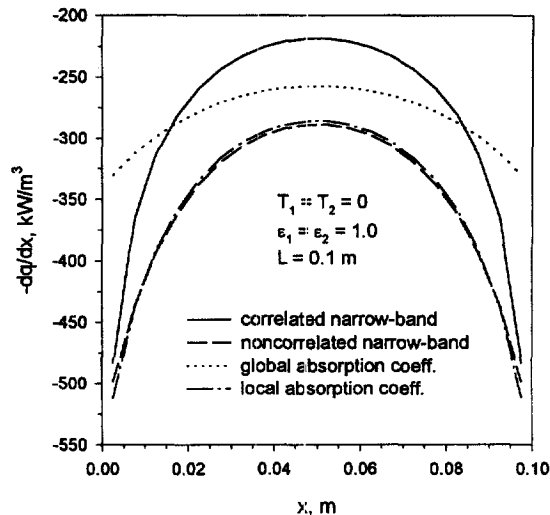
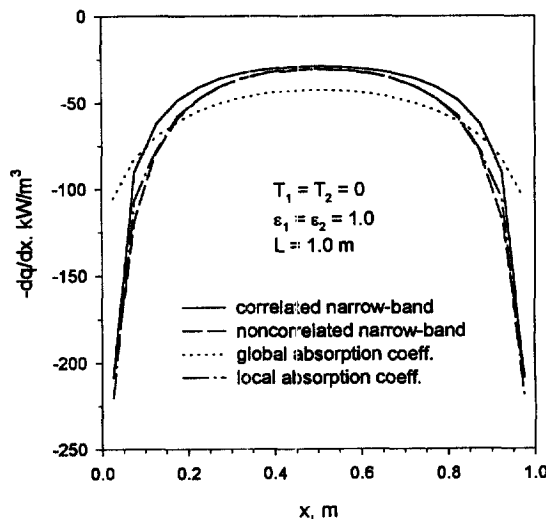
Figures 2 and 3 show the predicted radiative source distributions for the first test case with separation distances of  $0.1 \text{ m}$  and  $1 \text{ m}$ , respectively. A direct comparison between the results obtained from Methods I and III and those reported by Kim *et al.*

Table 1. Summary of the four test cases

Case	Species concentration profile	Temperature profile	$L$ [m]
1	Pure water vapour	Uniform	0.1 and 1
2	Parabolic $\text{H}_2\text{O}$ profile	Uniform	1
3	Pure water vapour	Boundary layer type	0.2
4	Simulated diffusion flame	Simulated diffusion flame	0.5

Table 2. Summary of the formulations for the four implementation methods

Method I	Correlated formulation, equation (4).
Method II	Noncorrelated formulation, equation (9).
Method III	Grey-band approximation, equation (10) with global $\bar{\kappa}$ , from equation (11).
Method IV	Grey-band approximation, equation (10) with local $\bar{\kappa}$ , from equation (15).

Fig. 2. Distribution of the predicted radiative source term for the uniform temperature profile:  $L = 0.1$  m.Fig. 3. Distribution of the predicted radiative source term for the uniform temperature profile:  $L = 1$  m.

[22] was not made since they used the older data set of the SNB model parameters published by Hartmann *et al.* [17] and Soufiani *et al.* [18]. However, the present results from these two methods are very close to those of Kim *et al.*

Results obtained from Methods II and IV are very close to each other with the results of Method IV

slightly better, compared to the results of Method I, in the middle of the enclosure and slightly worse near the walls. This is indeed expected since Method IV was derived from Method II and both methods made use of Beer's law.

For the smaller separation distance, Fig. 2, Methods II and IV underpredict the radiative source everywhere, especially in the middle of the enclosure. However, these two methods qualitatively predict the sharp variation of the radiative source distribution. Method III underpredicts the radiative source in the middle of the enclosure and greatly overpredicts it near the walls, i.e. this method gives flattened radiative source distribution. Kim *et al.* [22] attributed the poor performance of Method III to the step change between the wall and gas temperatures. However, it is believed that the failure of this method lies in the fact that equation (11) more severely underpredicts the equivalent absorption coefficient than equation (15) in this test case containing an isothermal and homogeneous medium. The radiative source distribution approaches a uniform profile,  $-\kappa_p \sigma T^4$ , in the optically thin limit.

For the larger separation distance, Fig. 3, Methods II and IV predict quite accurate radiative source distribution compared to the smaller separation distance case, Fig. 2. These results indicate that the 'history' effect is less significant in isothermal, homogeneous, and longer pathlength media. Again Method III predicts flattened radiative source distribution for the reason mentioned above.

The grid dependence of the numerical results of Method IV was investigated for case 1 with larger separation distance ( $L = 1$  m). The results are shown in Fig. 4. The use of five uniform gas layers results in nonphysical radiative source distribution. This can be attributed to the use of the diamond differencing scheme of DOM. It is well known that the diamond scheme yields oscillations in the intensity field when coarse grids are used. These nonphysical oscillations can be eliminated by using finer grids in one-dimension, which is evident in the results of Fig. 4. Figure 4 shows that the numerical results achieve grid independence rapidly as the number of gas layers increases and the use of 20 uniform gas layers is adequate.

Figure 5 shows the radiative source distribution predicted by the four methods for the second test case. Results of Methods II and IV are again very close to each other and in qualitative agreement with the benchmark solution, i.e. they correctly predict the 'w' shaped radiative source distribution revealed by Method I. The physical justification for the existence

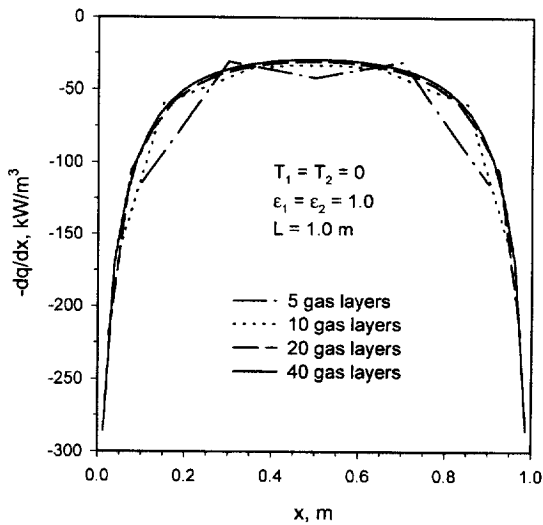


Fig. 4. Dependence of the numerical results of Method IV on the number of uniform gas layer for the uniform temperature profile:  $L = 1$  m.

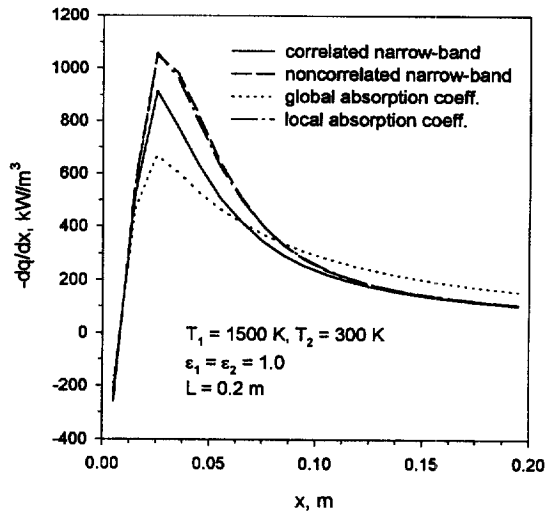


Fig. 6. Distribution of the predicted radiative source term for the boundary layer type temperature profile.

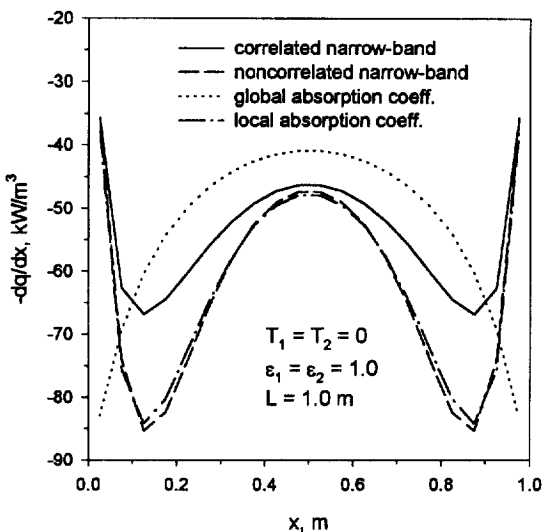


Fig. 5. Distribution of the predicted radiative source term for the parabolic  $H_2O$  concentration profile.

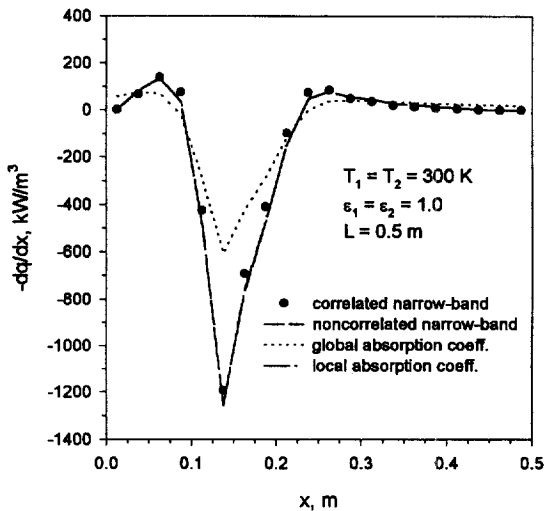


Fig. 7. Distribution of the predicted radiative source term for the simulated counterflow  $CH_4$ /air diffusion flame case.

of the 'w' shape in the radiative source distribution has been discussed by Kim *et al.* [22]. Errors of Methods II and IV are largest at the two valleys of the 'w' shape by as much as 27%. Method III fails to predict the 'w' shaped radiative source distribution exhibited from results of the other three methods. In fact, results of Method III are qualitatively similar to those for an isothermal and homogeneous medium shown in Figs. 2 and 3. This is also expected since Method III utilizes a spatially uniform absorption coefficient which certainly cannot capture any effects due to concentration distribution. Note that the temperature in this case is uniform.

The predicted radiative source distributions for

pure  $H_2O$  with a boundary layer type temperature variation (the third test case) are shown in Fig. 6. Results of Method II and IV are again in excellent agreement with each other. These two methods overpredict the radiative source term by about 16% at the peak of the curve. Method III fails to predict the sharp rise of the radiative source term near the hot wall and overpredicts it near the cold wall, as the consequence of using a global absorption coefficient.

Results for the simulated counterflow diffusion flame case are shown in Fig. 7. Results of Methods II and IV are almost identical and in good agreement with the result of Method I. Again, Method III cannot predict the deep valley in the radiative source distribution.

Numerical calculations were also performed by a

Table 3. Comparison of predicted net heat fluxes at the left wall (kW/m<sup>2</sup>)

Test case	Method I	Method II	Method III	Method IV
Case 1, $L = 0.1$ m	-14.2	-17.6	-14.1	-17.6
Case 1, $L = 1$ m	-30.3	-34.0	-29.9	-34.0
Case 2	-27.0	-31.2	-26.6	-31.1
Case 3	271.5	270.9	272.8	270.7
Case 4	-30.5	-34.9	-17.9	-34.8

Table 4. CPU time (seconds) consumed by four implementation methods of the SNB model in one-dimensional non-grey gas radiative transfer analyses

Grid number	Method I	Method II	Method III	Method IV
10	7.880	0.374	0.143	0.155
20	36.193	0.731	0.270	0.295
30	91.804	1.037	0.392	0.435
40	180.922	1.341	0.515	0.573
50	310.355	1.647	0.640	0.712
80	1009.226	2.563	1.102	1.130

thinner flame using similar temperature and species distributions given in Fig. 1 but nonuniform grid with smaller grids around the flame ( $x = 0.14$  m). Results of these calculations are qualitatively similar to those shown in Fig. 7 and can be briefly summarised as: (1) results of Methods II and IV are identical, (2) results of Methods II and IV are in even better agreement with the benchmark solution, (3) the radiative source term at the flame is much lower than that shown in Fig. 7, (4) Method III yields even more flattened radiative source distribution. These observations are the expected trends. For a very thin flame, the radiative source term from Methods I, II, and IV correctly approaches the optically thin limit,  $-\kappa_p \sigma T^4$ , while Method III predicts a uniform radiative source term of zero everywhere since the globally averaged absorption coefficient  $\bar{\kappa}_v$  approaches zero in the limit of a flame sheet.

Numerical results from this test case reveal that Methods II and IV predict fairly accurate radiative source term under conditions found in a typical counterflow diffusion flame. These methods can therefore be used in one-dimensional diffusion flame modelling with confidence.

Results from test cases containing nonisothermal and/or inhomogeneous media (Figs. 5–7) indicate that the correlation term in the correlated formulation tend to attenuate peaks and valleys in the radiative source distribution, i.e. it has smoothing effects compared to the noncorrelated formulation.

The predicted net heat fluxes at the left wall for the four test cases are compared in Table 3. Wall heat fluxes predicted by Methods II and IV are almost the same for all the cases. Method III predicts better wall

heat flux than the other two approximate methods, especially for the first two test cases; however, it predicts less accurate wall heat flux in the third and fourth cases, especially the fourth case. These results show that Method III predicts accurate wall heat fluxes for isothermal and homogeneous media, but less accurate for nonisothermal and inhomogeneous media. In fact, Method III should predict accurate wall heat flux, but not internal heat flux (or the radiative source term), for isothermal and homogeneous media since the grey-band absorption coefficient is formulated in terms of the mean pathlength of the enclosure.

Numerical calculations were also performed for different grid numbers using the four implementation methods to investigate their computational efficiency and the growth rate of CPU time with grid number. The results are summarised in Table 4. These calculations were conducted on a SGI Power Challenge (Model L) workstation. The correlated formulation requires two orders of magnitude more CPU time than the three approximate methods. In addition, the CPU time required by this method increases approximately with  $N^{2.3}$  ( $N$  is the grid number used in the calculation). The noncorrelated formulation requires about twice CPU time as the two grey-band approximations. CPU time of the three approximate methods grows with a sub-linear rate. Therefore more CPU time is saved using the three approximate methods when a large number of grids is required in the calculation.

#### 4. CONCLUSIONS

An alternative grey-band approximation was proposed for implementing the statistical narrow-band

model in non-grey gas radiative transfer analyses. This grey-band approximation was derived from the non-correlated formulation along with Beer's law. Theoretical analyses showed that the equivalent narrow-band absorption coefficient of the grey-band approximation method should be calculated using the local properties rather than global ones.

Non-grey gas radiation analyses using the statistical narrow-band model with an updated data set were performed in one-dimensional parallel plates enclosure containing radiating gases with different distributions in temperature and species concentration. Four implementation methods of the narrow-band model were used to perform the calculations: the exact or the correlated method for providing benchmark solutions and three approximate methods, the non-correlated formulation and two grey-band approximations using, respectively, global and local absorption coefficients. Accuracy of the three approximate methods was investigated for four test cases by comparing their results to the benchmark solutions. The grey-band approximation using local absorption coefficient and the noncorrelated formulation yield almost the same results for all the test cases. Results of these two methods are in fair to good agreement with the benchmark solutions. The radiative source terms predicted from the grey-band approximation using global absorption coefficient are shown to have serious errors. CPU time savings of two orders of magnitude can be achieved using the three approximate methods. Although the grey-band approximation using local absorption coefficient does not offer significantly better accuracy than the non-correlated formulation, it is more attractive in multi-dimensional applications since an arbitrary solution method can be readily used and about half computational effort is required. The present method is therefore promising for multidimensional non-grey gas radiation analyses and demands further investigation.

*Acknowledgements*—Financial support from the Department of National Defence of Canada is gratefully acknowledged. The authors are grateful to Dr A Soufiani of Ecole Centrale de Paris, EM2C, who generously provided the updated data set of the statistical narrow-band model parameters.

## REFERENCES

- Ronney, P. D., On the mechanisms of flame propagation limits and extinguishment processes at microgravity. *22nd Symp. (Int.) on Combustion*. The Combustion Institute, 1988, pp. 1615–1623.
- Sibulkin, M. and Frendi, A., Prediction of flammability limit of an unconfined premixed gas in the absence of gravity. *Combust. Flame*, 1990, **82**, 334–345.
- Daguse, T., Croonenbroek, T., Rolon, J. C., Darabiha, N. and Soufiani, A., Study of radiative effects on laminar counterflow  $H_2/O_2/N_2$  diffusion flames. *Combust. Flame*, 1996, **106**, 271–287.
- Guo, H., Ju, Y., Maruta, K., Niiooka, T. and Liu, F., Radiation extinction limit of counterflow premixed lean methane–air flames. *Combust. Flame*, 1997, **109**, 639–646.
- Ju, Y., Guo, H., Maruta, K. and Liu, F., On the extinction limit and flammability limit of non-adiabatic stretched methane–air premixed flame. *Journal of Fluid Mechanics*, 1997, to appear.
- Ju, Y., Guo, H., Maruta, K. and Niiooka, T., Flame bifurcations and flammable regions of radiative counterflow premixed flames with general Lewis numbers, submitted to *Combust. Flame*, 1997.
- Abbud-Madrid, A. and Ronney, P. D., Premixed flame propagation in an optically thick gas. *AIAA Journal*, 1993, **31**, 2179–2981.
- Mengüç, M. P. and Viskanta, R., An assessment of spectral radiative heat transfer predictions for a pulverized coal-fired furnace. *Proceedings of the Eighth International Heat Transfer Conference*, Vol. 2. San Francisco, 1986, pp. 815–820.
- Goody, R. M. and Yung, Y. L., *Atmospheric Radiation*, 2nd edn. Oxford, U.K., 1989.
- Goody, R., West, R., Chen, L. and Chrisp, D., The correlated- $k$  method for radiation calculations in non-homogeneous atmospheres. *J. Quant. Spectroscopy Radiative Transfer*, 1989, **42**, 539–550.
- Soufiani, A., Gas radiation spectral correlated approaches for industrial applications. In *Heat Transfer in Radiating and Combusting Systems*, ed. M. G. Carvalho, F. Lockwood and J. Taine. Springer-Verlag, 1991.
- Denison, M. K. and Webb, B. W., A spectral line-based weighted-sum-of-grey-gases model for arbitrary RTE solvers. *ASME Journal of Heat Transfer*, 1993, **115**, 1004–1012.
- Denison, M. K. and Webb, B. W., An absorption-line blackbody distribution function for efficient calculation of gas radiative transfer. *J. Quant. Spectroscopy Radiative Transfer*, 1993, **50**(2), 243–257.
- Denison, M. K. and Webb, B. W., Development and application of an absorption-line blackbody distribution function for  $CO_2$ . *International Journal of Heat and Mass Transfer*, 1995, **38**(10), 1813–1821.
- Denison, M. K. and Webb, B. W., The spectral line-based weighted-sum-of-grey-gases model in non-isothermal non-homogeneous media. *ASME Journal of Heat Transfer*, 1995, **117**(2), 339–365.
- Liu, J., Shang, H. M., Chen, Y. S. and Wang, T. S., GRASP: a general radiation simulation program. *32nd Thermophysics Conference*, AIAA 97-2559, Atlanta, GA, 1997.
- Hartmann, J. M., Levi Di Leon, R. and Taine, J., Line-by-line and narrow-band statistical model calculation for  $H_2O$ . *J. Quant. Spectroscopy Radiative Transfer*, 1984, **32**(2), 119–127.
- Soufiani, A., Hartmann, J. M. and Taine, J., Validity of band-model calculations for  $CO_2$  and  $H_2O$  applied to radiative properties and conductive–radiative transfer. *J. Quant. Spectroscopy Radiative Transfer*, 1985, **33**(3), 243–257.
- Zhang, L., Soufiani, A. and Taine, J., Spectral correlated and non-correlated radiative transfer in a finite axisymmetric system containing an absorbing and emitting real gas-particle mixture. *International Journal of Heat and Mass Transfer*, 1985, **31**, 2261–2272.
- Soufiani, A. and Taine, J., High temperature gas radiative property parameters of statistical narrow-band model for  $H_2$ ,  $CO_2$  and  $CO$  and correlated- $K$  (CK) model for  $H_2O$  and  $CO_2$ . *International Journal of Heat and Mass Transfer*, 1997, in press.
- Liu, F., A ray-tracing method for solving the radiative transfer equation in three-dimensional participating media, submitted to *ASME Journal of Heat Transfer*, 1997.

22. Kim, T.-K., Menart, J. A. and Lee, H. S., Nongray radiative gas analysis using the S-N discrete ordinates method. *ASME Journal of Heat Transfer*, 1991, **113**, 946–952.
23. De Miranda, A. B. and Sacadura, J. F., An alternative formulation of the S-N discrete ordinates for predicting radiative transfer in nongrey gases. *ASME J. Heat Transfer*, 1996, **118**, 650–653.
24. Edwards, D. K., Molecular gas band radiation. *Advances in Heat Transfer*, Vol. 12. Academic Press, New York, 1976, pp. 115–193.
25. Carlson, B. G. and Lathrop, K. D., Transport theory—the method of discrete ordinates. In *Computing Method in Reactor Physics*, ed. H. Greenspan, C. N. Keller and D. Okrent. Gordon and Breach, New York, 1968.
26. Siegel, R. and Howell, J. F., *Thermal Radiation Heat Transfer*, 2nd edn. Hemisphere, 1981.
27. Menart, J. A., Lee, H. S. and Kim, T.-K., Discrete ordinates solution of nongrey radiative transfer with diffusely reflecting walls. *ASME Journal of Heat Transfer*, 1993, **115**, 184–193.
28. Fiveland W. and Jamaluddin, A. S., Three-dimensional spectral radiative heat transfer solutions by the discrete-ordinates method. *Journal of Thermophysics*, 1991, **5**(3), 335–340.
29. Hottel, H. C. and Sarofim, A. F. *Radiative Transfer*. McGraw-Hill, 1967.
30. Ludwig, D. B., Malkmus, W., Reardon, J. E. and Thomson, J. A. L., *Handbook of Infrared Radiation from Combustion Gases*. NASA SP3080, 1973.
31. Soufiani, A., Private communication, January 1997.
32. Liu, J. and Tiwari, S. N., Investigation of radiative transfer in nongrey gases using a narrow band model and Monte Carlo simulation. *ASME Journal of Heat Transfer*, 1994, **116**, 160–166.
33. Thurgood, C. P., Pollard, A. and Becker, H. A., The  $T_N$  quadrature set for the discrete ordinates method. *ASME Journal of Heat Transfer*, 1995, **117**, 1068–1070.